Scheme I

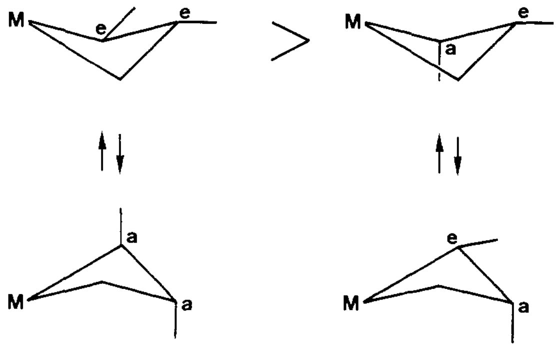

Scheme II

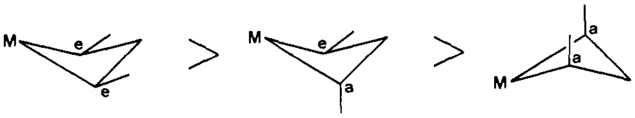

Table I. Effect of Methyl Substituents in the 1-2-Positions on Total Energy (eV) of Metallacyclobutane

	puckering angle, deg				
	M = W			M = Cr	
conformation	0	12	40	0	12
1e–2a[a]	−1155.19	−1153.26	−1148.84	−1154.22	−1153.28
1a–2e[a]	−1155.19	−1155.99	−1157.05	−1154.22	−1154.45
1a–2a[b]	−1157.72	−1155.45	−1151.10	−1156.52	−1154.19
1e–2e[b]	−1157.72	−1158.60	−1158.74	−1156.52	−1157.63

[a] Cis-directing conformation. [b] Trans-directing conformation.

Table II. Effect of Methyl Substituents in the 1–3-positions on Total Energy (eV) of Metallacyclobutane

	puckering angle, deg				
	M = W			M = Cr	
conformation	0	12	40	0	12
1e–3a[a]	−1157.02	−1157.03	−1156.86	−1153.91	−1153.99
1a–3a[b]	−1156.97	−1156.63	−1155.49	−1153.81	−1152.89
1e–3e[b]	−1156.97	−1157.31	−1157.71	−1153.81	−1154.89

[a] This conformation *does not result* in a retention of the configuration of the starting *cis*- or *trans*-olefin. [b] These conformations *result* in a retention of the configuration of the starting *cis*- or *trans*-olefin.

Table III. Effect of Methyl Substituent in the 1-Position and Ethyl Substituent in the 3-Position on Total Energy (eV) of Metallacyclobutane (M = W)

	puckering angle, deg		
conformation	0	10	20
1Mee-3Eta[a]	−1263.67	−1263.71	−1263.79
1Mea-3Ete[a]	−1263.67	−1263.70	−1263.79
1Mea-3Eta[b]	−1263.62	−1263.35	−1263.11
1Mee–3Ete[b]	−1263.62	−1263.95	−1264.30

[a] These conformations *do not result* in a retention of the configuration of the starting *cis*- or *trans*-olefin. [b] These conformations *result* in a retention of the configuration of the starting *cis*- or *trans*-olefin.

$Cp_2\underline{TiCH_2CRR'CH_2}$[10] or $L_2Cl_2\underline{PtCH_2CH_2CH_2}$.[7]

It has been postulated that the trans stereoselectivity observed in metathesis of α-olefins was due to the favored 1–2 e–e conformation with respect to the 1–2 a–e conformation of the substituted metallacycle[5,6] (Scheme I).

Calculations (Table I) are in agreement with such prediction since the most stable conformation is the e–e one. Besides, the planar conformation appears not to be the most stable one.

The retention of configuration of the starting olefin in metathesis of acyclic olefins is usually ascribed to the occurence of a 1–3 diaxal interaction[1–6] (Scheme II).

By comparing the stabilities of the planar and puckered conformations, it appears that the most stable one is the puckered 1e–3e conformation (Tables II and III).

In group 6, chromium-based catalysts are more stereoselective than molybdenum-based catalysts, which are more stereoselective than tungsten-based catalysts.[5] This effect has been tentatively explained on the basis of the decrease of the M–C distance of the metallacycle in the order W > Mo > Cr. A simultaneous increase in the 1–3 interaction would result from such shortening of the M–C σ-bond. This trend is also apparent from the calculations: the energy difference between the 1e–3e and the 1e–3a conformation is more pronounced with chromium than with tungsten. It appears also that regardless of their conformations, chromiacyclobutanes are less stable than tungstacyclobutanes, which is in rough agreement with ab initio calculations of Goddard carried out with similar systems.[17,18]

In conclusion, from these extended Hückel calculations it appears that (i) the presence of substituents in a metallacycle of the type $Cl_4\underline{MCHR_1CHR_2CHR_3}$ will favor a puckered conformation, (ii) with a 1–2-substituted metallacycle, the favored conformation is the 1e–2e one, (iii) with a 1–3-substituted metallacycle, the favored conformation is the 1e–3e one, (iv) the 1–2 interactions, which favor the formation of trans products regardless of the cis or trans nature of the starting olefin, are more pronounced than the 1–3 interactions, in good agreement with Calderon's experiments with very bulky olefins,[6] and (v) the effects are more pronounced with chromium than with tungsten.

These results are in good qualitative agreement with the results of the literature concerning the stereochemistry of metathesis of internal or terminal olefins. Further studies are in progress to investigate simultaneously those effects in the case of *cis*- and *trans*-2-pentene[5] as well as *cis*- or *trans*-4-methyl-2-pentene metathesis.[6]

---

[17] A. K. Rappe and W. A. Goddard III, *J. Am. Chem. Soc.*, **102**, 5114 (1980).

[18] A. K. Rappe and W. A. Goddard III, *J. Am. Chem. Soc.*, **104**, 448 (1982).

Surface Acid Site Characterization by means of CP/MAS Nitrogen-15 NMR

John A. Ripmeester

Division of Chemistry
National Research Council of Canada
Ottawa, Ontario K1A 0R9, Canada

Received October 18, 1982

The surface properties of heterogeneous solids with catalytic activity are of continuing interest with respect both to the nature of the active sites and to how these sites are modified by chemical or physical treatment. The presence of both Brønsted and Lewis acid sites in solid catalysts has been inferred from infrared spectroscopic studies,[1–3] and attemps have been made to study such active sites by means of ^{1}H[3] and ^{13}C NMR.[4,5] On considering the large nuclear shielding range that ^{15}N NMR presents,[6] use of this nucleus becomes an attractive possibility in studies of this

---

(1) S. M. Riseman, F. E. Massoth, G. M. Dhar, and E. M. Eyring, *J. Phys. Chem.*, **86**, 1760 (1982).

(2) F. R. Cannings, *J. Phys. Chem.*, **72**, 4691 (1968).

(3) L. Petrakis and F. E. Kiviat, *J. Phys. Chem.*, **80**, 606 (1976).

(4) (a) W. H. Dawson, S. W. Kaiser, P. D. Ellis, and R. R. Inners, *J. Am. Chem. Soc.*, **103**, 6780 (1981). (b) W. H. Dawson, S. W. Kaiser, P. D. Ellis, and R. R. Inners, *J. Phys. Chem.*, **86**, 867 (1982).

(5) (a) S. H. C. Liang and I. D. Gay, *J. Catal.*, **66**, 249 (1980). (b) I. D. Gay and S. Liang, *ibid.*, **44**, 306 (1976). (c) I. D. Gay, *ibid.*, **48**, 430 (1977).

(6) M. Witanowski, L. Stefaniak, and G. A. Webb, *Annu. Rep. NMR Spectrosc.*, **7**, 117 (1977).

0002-7863/83/1505-2925$01.50/0 Published 1983 by the American Chemical Society

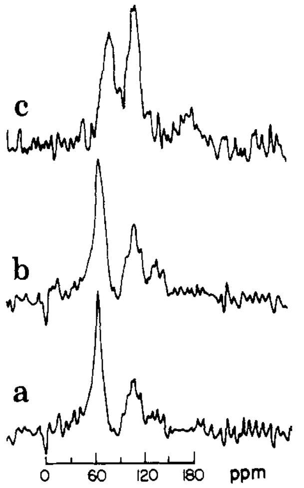

Figure 1. ^{15}N CP/MAS spectrum of pyridine-^{15}*N* sorbed on γ-alumina: (a) after 2 h of accumulation; (b) after 4 h of accumulation; (c) sample exposed to air for 2 h, 15000 scans.

Table I. Nitrogen Chemical Shifts for Pyridine and Sorbed Pyridine

pyridine[a]	
neat	+58
aqueous	+80
in 10 M HCl	+175
pyridine on γ-alumina[b]	
physically sorbed	+64
physically sorbed and hydrated	+76
Lewis acid site I	+110
Lewis acid site II	+138
pyridinium ion	+174
pyridine on mordenite[b]	
physically sorbed in channels	+84
Lewis acid	+121
Brønsted acid (pyridinium ion)	+171

[a] From ^{14}N chemical shift data; reference, saturated aqueous NH_4NO_3. [b] ^{15}N shifts are reported with respect to solid NH_4NO_3. Solid and solution chemical shifts for NO_3^- differ by no more than 1 ppm.

nature, and indeed two high-resolution ^{15}N NMR studies dealing with adsorbed species have recently appeared.[7] Because of the low sensitivity of natural abundance ^{15}N NMR and the small quantities of material involved it is well worthwhile to use highly enriched materials. Results presented here, obtained for pyridine-^{15}*N* sorbed on γ-alumina and mordenite samples, show that several kinds of sorbed pyridine may be identified by means of CP/MAS ^{15}N NMR.

Figure 1, parts a and b, shows the ^{15}N NMR spectrum[9] of pyridine-^{15}*N* sorbed on γ-alumina.[8] Three relatively broad lines are evident at 64, 110, and 138 ppm (see Table I). The low-field line was observed to broaden as the spectral accumulation continued: spectrum 1a was obtained after ~2 h of accumulation, spectrum 1b after ~4 h. From the chemical shift of this line, it can be associated with physisorbed pyridine, which slowly picked up water, as evidently the spinner caps were not tight enough to exclude air and moisture completely (air was used as driving fluid for the spinner). On deliberate exposure to air the line shifts further to 78 ppm (Figure 1c), in agreement with a hydration hypothesis. There is no evidence for protonated pyridine on initial exposure of γ-alumina to pyridine vapor, as there is no visible absorption at ~170 ppm. The other two lines can therefore be assigned to coordinately bound pyridine, i.e., Lewis acid sites. It is of interest to note that the line at 138 ppm disappears on exposure of the sample to air, whereas the line at 110 ppm does not appear to change. Hence, the Lewis acid complex corresponding to the high-field line apparently is unstable in the presence of water, perhaps because of a preferential interaction of water molecules with the active center. Figure 1c also shows there to be a weak absorption at ~174 ppm, attributable to pyridinium ions. It is pertinent to note that in a recent ^{13}C NMR study[4b] of pyridine on γ-alumina, absorption at ~168 ppm was attributed to carbonate or bicarbonate species, which appeared after exposure of the sample to air. The protonated pyridine may well be the counterion of such species.

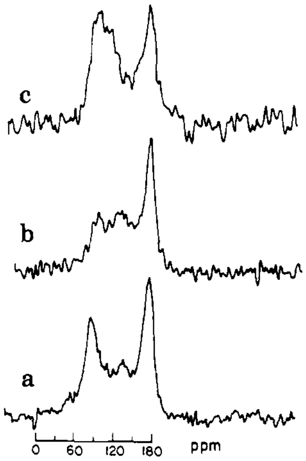

Figure 2. ^{15}N CP/MAS spectrum of pyridine-^{15}*N* sorbed on acid-leached calcined mordenite: (a) fresh sample; (b) sample purged with dry nitrogen; (c) sample exposed to air for ~2 h, 12000 scans.

The ^{13}C NMR study[4b] of pyridine sorbed on γ-alumina also showed that the pyridine ^{13}C chemical shifts were near to those expected for liquid pyridine. Evidence for a complex formation and changes therein on interaction of the sample with moist air were inferred from relative changes in line intensities.

The spectrum of pyridine-^{15}*N* sorbed on an acid-leached, calcined sodium mordenite sample is shown in Figure 2a. Three broad lines can be seen at 84, 121, and 171 ppm. On purging the sample with dry nitrogen, the line at 84 ppm has reduced intensity and can be assigned to pyridine sorbed physically in the mordenite channels. The high-field line at ~171 ppm can again be assigned to protonated pyridine, this time associated with Brønsted acid sites. The third broad line centered at ~121 ppm can be associated with a Lewis acid site. On exposure to moist air, this broad line disappears, and there appears to be increased intensity near 110 ppm. Apparently water interacts preferentially with the Lewis acid site, or perhaps a different complex species is formed involving the surface, water, and pyridine.

^{15}N NMR appears to be better suited for the identification of surface sites than ^{13}C NMR. In this study, four distinct types of pyridine molecules were found to be associated with the γ-alumina surface, whereas only a single type of pyridine was identified by means of ^{13}C NMR.[4b] In agreement with recent infrared work,[1] two distinct pyridines could be assigned to Lewis acid sites. It should again be emphasized that spectra obtained by means of cross-polarization techniques require the presence of nonzero ^{1}H-rare nucleus dipole–dipole coupling. This implies that molecular motion of the molecule observed must be anisotropic and in the slow-diffusion limit. The observation of separate signals for different pyridine species indicates also that chemical exchange is slow, although there may be a contribution to the line width from slow exchange processes.

---

(7) (a) T. Bernstein, L. Kitaev, D. Michel, H. Pfeifer, and P. Fink, *J. Chem. Soc., Farad. Trans. 1*, **78**, 761 (1982). (b) D. Michel, A. Germanus, and H. Pfeifer, *J. Chem. Soc., Farad Trans. 1*, **78**, 237 (1982).

(8) γ-Alumina was prepared by heating bohmite at 450 °C for 24 h. Sodium mordenite was leached with hot 8 N HCl for 24 h, washed, dried, and calcined in air at 500 °C for 24 h (see, for example, W. L. Kranich, Y. H. Ma, L. B. Sand, A. H. Weiss, and I. Zwiebel, *Adv. Chem., Ser.*, No. **101**, 502 (1971)). Each sample was heated to 300 °C under vacuum immediately before exposure to pyridine-^{15}*N* vapor. Adsorption was considered to be complete after exposure times of ~12 h. Samples were transferred to Delrin rotors under dry nitrogen.

(9) ^{15}N NMR spectra were obtained at 18.25 MHz on a Bruker CXP-180 NMR spectrometer. Cross-polarization times were 1 ms, recycle times 2 s. Matched radio-frequency amplitudes were 28 kHz. Chemical shifts were measured with respect to the nitrate line of solid external NH_4NO_3: ($|\delta_{(NO_3^-)} - \delta_{(NH_4^+)}| = 353.7$ ppm).

The results presented here also indicate that high-resolution techniques are not able to give information on the sites identified by CP/MAS NMR, as there is no, or very slow, exchange between these species and the more mobile species visible to the high-resolution NMR experiment even in samples loaded to maximum capacity with pyridine. One reason may be the very large shielding anisotropy of ^{15}N in pyridine,[10] so that any slow anisotropic motions of the adsorbed molecules lead to severe line broadening.

Registry No. ^{15}N, 14390-96-6; Al_2O_3, 1344-28-1; mordenite, 12173-98-7; pyridine, 110-86-1.

---

(10) The shielding tensor for ^{15}N in solid pyridine has been reported to be $\sigma_{xx} = -313$, $\sigma_{yy} = -94$, and $\sigma_{zz} = 469$ ppm: D. Schweitzer, H. W. Spiess, *J. Magn. Reson.*, **15**, 529 (1974). Preliminary measurements indicate that the Brønsted acid pyridine-^{15}N site in the mordenite sample has an axially symmetric shielding tensor with $\Delta\sigma \sim 270$ ppm.

A New Class of σ-Bonded Aliphatic Aza-Macrocyclic Complexes of Transition Metals: Synthesis and X-ray Crystal Structures of Nitrogen-Bridged $[(TiN_4C_{12}H_{24})_2]$ and Oxo-Bridged $[(N_4C_{12}H_{25})TiOTi(N_4C_{12}H_{25})]$[†]

Marilyn M. Olmstead, Philip P. Power,* and
Michael Viggiano

Department of Chemistry, University of California, Davis
Davis, California 95616

Received January 17, 1983

Transition-metal complexes having aliphatic macrocyclic ligands with several nitrogen donor atoms have been intensively investigated over the past 20 years.[1] In the saturated macrocyclic ligands the ring nitrogens are usually secondary, and two types of metal–nitrogen bonding are possible. These are (a) each nitrogen behaves as a classical two-electron donor, exemplified by M ← :N(H)<, resulting in the formation of an amine complex or (b) each nitrogen σ-bonds to the metal, as shown by M–N̈<, giving an amide complex. Only complexes of type a have been reported in the literature. During the course of our attempts to induce unusual early-transition-metal geometries with these macrocycles, we have isolated the first examples of type b complexes. These are (i) the dimeric d^0 titanium(IV) derivative of 1,5,9,13-tetraazacyclohexadecane $[(TiN_4C_{12}H_{24})_2]$ (**1**), and (ii) the μ-oxo-bridged species formed via the reaction of **1** with water, $[O(TiN_4C_{12}H_{25})_2]$ (**2**).

Compounds **1** and **2** were synthesized in good yield by Scheme I.

The structures of **1**[2a] and **2**[2b] possess several unique features and are illustrated in Figures 1 and 2. For **1** the X-ray crystal structure is the first reported for a homoleptic titanium(IV) dialkylamide. The geometry at Ti is distorted trigonal bipyramidal and a rare example of five-coordinate Ti(IV).[3] The terminal nitrogens, N(2), N(3), and N(4), possess near-planar geometry, and the average Ti–N distance, 1.94 Å, is close to the value found in other Ti(IV) amides.[4] The Ti–N bonds involved in bridging have the longer values of 2.191 (2) Å for Ti–N(1) and 2.147 (2) Å for Ti–N(1)′. The Ti···Ti distance, 3.380 (1) Å, precludes significant metal–metal interactions. The dimeric structure is similar to that proposed by Richman for the strained cyclic 12- and 13-membered ring systems PN_4^+ on the basis of ^{31}P and ^{13}C NMR spectroscopy.[5,6] In the phosphorus system dimerization is seen only if the geometry is constrained by ring size. Monomeric species are obtained if the size of the ring is increased to a 16-membered ring for phosphorus. The dimerization seen in **1** probably reflects the relatively larger size of titanium.

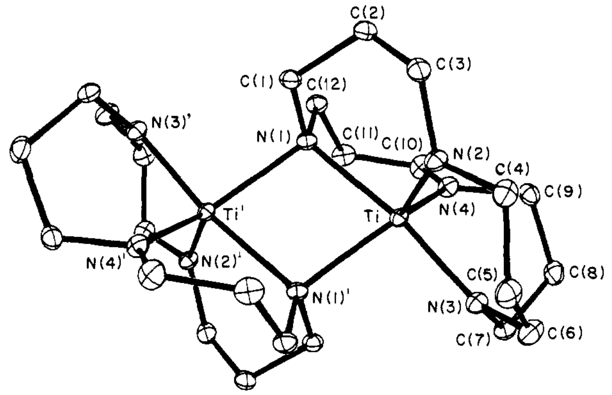

Figure 1. Computer-generated representative diagram of $[(TiN_4C_{12}H_{24})_2]$, **1**. Important bond distances (Å) and angles (deg) are Ti–N(1) = 2.191 (2), Ti–N(2) = 1.928 (2), Ti–N(3) = 1.947 (2), Ti–N(4) = 1.943 (3), Ti–N(1)′ = 2.147 (2); N(1)–Ti–N(3) = 167.1 (1), N(2)–Ti–N(4) = 115.3 (1), N(1)′–Ti–N(2) = 115.3 (1), N(1)′–Ti–N(4) = 128.6 (1), Ti′–N(1)–Ti = 102.4 (1), and N(1)–Ti–N(1)′ = 77.6 (1).

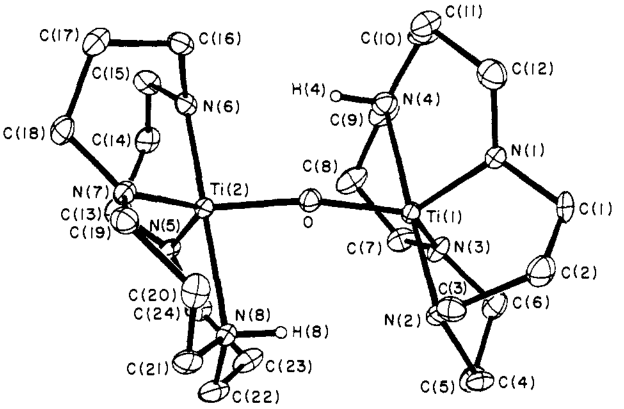

Figure 2. Computer-generated representative diagram of $[O(TiN_4C_{12}H_{25})_2]$, **2**. Important bond distances (Å) and angles (deg) are Ti(1)–N(1) = 1.942 (4), Ti(1)–N(2) = 1.962 (4), Ti(1)–N(3) = 1.941 (4), Ti(1)–N(4) = 2.283 (4), Ti(1)–O = 1.838 (3); Ti(1)–O–Ti(2) = 152.0 (2), N(1)–Ti(1)–N(3) = 117.4 (2), N(2)–Ti(1)–N(4) = 178.7 (1), N(1)–Ti(1)–O = 114.4 (1), and N(3)–Ti(1)–O = 126.7 (2). The angles and distances surrounding Ti(2) are similar to those above.

Scheme I

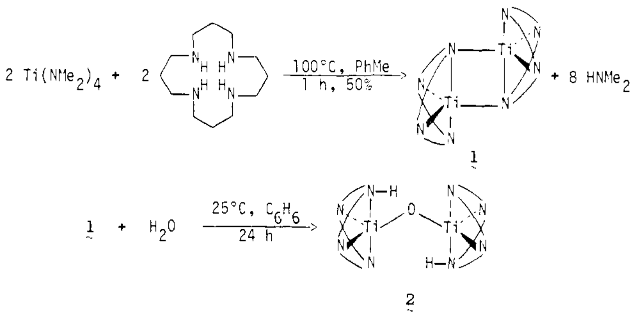

[†] No reprints available.

(1) Melson, G. A. "Coordination Chemistry of Macrocyclic Compounds"; Plenum Press: New York, 1979. Izatt, R. M.; Christensen, J. J. "Synthetic Multidentate Macrocyclic Compounds"; Academic Press: New York, 1978.

(2) (a) Crystal data for **1** at 140 K with Mo Kα radiation (λ 0.71069 Å): triclinic, $P\bar{1}$ (no. 2); $a = 8.500$ (2) Å, $b = 9.282$ (2) Å, $c = 9.312$ (3) Å; $\alpha = 98.45$ (2)°, $\beta = 115.69$ (2)°, $\gamma = 90.95$ (2)°; $Z = 1$; $\mu = 6.33$ cm^{-1}; 2552 unique observed data, 250 parameters; $R = 0.044$. (b) **2**: triclinic, $P\bar{1}$, (no. 2); $a = 9.435$ (2) Å, $b = 11.280$ (3) Å, $c = 14.036$ (3) Å; $\alpha = 84.88$ (2)°, $\beta = 84.22$ (2)°, $\gamma = 69.69$ (2)°; $Z = 2$; $\mu = 5.98$ cm^{-1}, 3826 unique observed data, 324 parameters; $R = 0.059$.

(3) Dwyer, P. D.; Puppe, L.; Bushler, J. W.; Scheidt, W. R. *Inorg. Chem.* **1975**, *14*, 1782–1786.

(4) Lappert, M. F.; Power, P. P.; Sanger, A. R.; Srivastava, R. C. "Metal and Metalloid Amides"; Horwood-Wiley: Chichester, 1978.

(5) Richman, J. E.; Gupta, O. D.; Flay, R. B. *J. Am. Chem. Soc.* **1981**, *103*, 1291–1292.

(6) Richman, J. E.; Day, R. O.; Holmes, R. R. *J. Am. Chem. Soc.* **1980**, *102*, 3955–3956.

0002-7863/83/1505-2927$01.50/0